Heliyon 9 (2023) e18648

Contents lists available at ScienceDirect

Heliyon

journal homepage: www.cell.com/heliyon

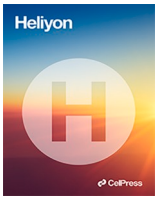

Assessment of soil erosion hazard and its relation to land use land cover changes: Case study from alage watershed, central Rift Valley of Ethiopia

Gebeyehu Taye [a,c,*], Tesfaye Teklesilassie [b,c], Daniel Teka [a,c], Henok Kassa [d,e]

[a] Department of Land Resource Management and Environmental Protection, Mekelle University, P. O. Box 231, Mekelle, Ethiopia
[b] Department of Natural Resource Management, Dilla University, P. O. Box 419, Dilla, Ethiopia
[c] Institutes of Geoinformation and Earth Observation Sciences, Mekelle University, P.O.Box 231, Mekelle, Ethiopia
[d] Department of Natural Resources Management, Mizan-Tepi University, PO Box 260, Mizan-Tepi, Ethiopia
[e] Department of Ecology, Biogeochemistry and Environmental Protection, University of Wrocław, Wrocław, Poland

ARTICLE INFO

Keywords:
Soil loss
Land use land cover change
Revised universal soil loss equation
Rift Valley
Ethiopia

ABSTRACT

Soil erosion by water and wind is among the most crucial land degradation processes in Ethiopia. This is also the case for Alage watershed located in the cental Rift Valley system. This study aimed at assessment of soil erosion hazard and its relation to land use land cover change in the watershed during the period from 1984 to 2016 for a better land management. The study is based on application of Remote Sensing (RS) and Geographical Information System (GIS) to extract inputs factor values for the Revised Universal Soil Loss Equation (RUSLE). Time-series satellite imageries of Landsat TM 1984, ETM+ 2000 and OLI 2016 were used for land use land cover change detection and determination of cover management (C) factor of the RUSLE. Biophysical data such as rainfall, soil properties, land management practices including soil and water conservation measures within the watershed were collected using field survey and secondary data sources. Slope steepness and slope length factors were derived using Digital Elevaition Model (DEM). Long-term average annual soil loss rates were estimated by the RUSLE integrated with GIS for 1984, 2000 and 2016. Using satellite imageries, the land use land cover and changes within the watershed during the three periods were obtained through a supervised classification with maximum likelihood algorithim. The results of land use land cover change indicated that the proportion of rain-fed cropland, bare land and built up areas increased by 17.4%, 5.9% and 2.9% respectively over the three study period. In contrast the proportion of bush/shrub land, irrigated cropland, grass land, forested areas and waterbodies decresaed by 15.5%, 4.7%, 3.4%, 2.3% and 0.3% respectively during the same period. Estimated average annual soil loss rates showed an increasing trend from 24.3 ton ha^{-1} yr^{-1} in 1984 to 38 ton ha^{-1} yr^{-1} in 2016. Increasing trends of average annual soil loss rate is attributed to increased proportion of cropland, bare land and built up areas during those periods leading to decreased protective vegetation cover. Hotspot areas within the watershed require implementation of land management practices to prevent further degradation and expansion of gullies. This study is relevant to demonstrate environmental implication of land use land cover change for future land management practices and land use policy in the Rift Valley of central Ethiopia.

* Corresponding author. Department of Land Resource Management and Environmental Protection, Mekelle University, P. O. Box 231, Mekelle, Ethiopia.
E-mail address: gebeyehu.taye@mu.edu.et (G. Taye).

https://doi.org/10.1016/j.heliyon.2023.e18648
Received 1 January 2023; Received in revised form 23 July 2023; Accepted 24 July 2023
Available online 27 July 2023

1. Introduction

Soil erosion caused by water and wind is the most important process of land degradation globally [1–5]. While soil erosion is a natural geomorphic processes, its rate is accelerated by human land use systems involving overgrazing, deforestation and land use conversion [3,6–8]. Especially in the dryland environments, such accelerated soil erosion is a major threat to agricultural production through the physical removal of productive topsoil, loss of soil nutrients and productive water resources [4,6,9,10]. Eroded sediment is exported from agricultural watersheds and finally deposited in reservoirs and lakes, reducing their water storage capacity [5,11–13]. This siltation imposes an important threat to reservoirs affecting their intended purposes such as the potentials for irrigation, aquaculture, hydropower or recreational values over time [13,14]. In addition to sedimentation of reservoirs, sediment and sediment fixed nutrient export from agricultural watersheds is also an important sources of nutrients for eutrophication leading to algae bloom and disruption of the functioning of aquatic ecosystem [15–17].

A quantitative assessment of soil erosion rates and its consequence is needed for the planning and implementation of soil and water management and ecological rehabilitation interventions [8,18]. Several approaches have been proposed to measure and understand the rates of soil erosion so that effective conservation strategies can be implemented to curb soil erosion and restore degraded areas [19,20]. This is particularly relevant where lack of appropriate land management practices, rapid population growth, land use land cover change and related land degradation processes are the most widespread environmental problems. This is also the case in the arid and semi-arid Ethiopian highlands [7,21–24]. Land use land cover change in Ethiopian highlands, is accelerated due to population pressure and cropland expansion at the expense of forest, grassland and bush/shrub land [24,25]. This land use conversion on the hillslopes followed by agricultural intensification leads to accelerated water erosion hazard and soil fertility depletion [26–28]. Hence, assessment of erosion hazard from large area such as watersheds and understanding its association to land use land cover change using soil erosion models is crucial for proposing better land use and conservation planning and land use policy [20,26,29].

Several studies have already been conducted to assess soil erosion and sediment export rate in Ethiopian highlands at different spatial and temporal scales e.g. [14,22,26,30–33]. Reported soil loss values in Ethiopia vary over a wide range due to differences in measurement scales, applied methods, variation in climate, land use and soil types. Nevertheless, most of these reported values are larger than the proposed soil loss tolerance of 2–18 ton ha^{-1} yr^{-1} for Ethiopia [8]. This soil erosion rates have led to declining in soil fertility, its water holding capacity and crop productivity [28,34,35]. As a consequence of the increased rates of soil erosion, natural and constructed water harvesting reservoirs located in the downstream are silted up and water quality is deteriorating [13,15].

Similarly, accelerated soil erosion in the central Rift Valley has resulted into declining of agricultural productivity, deterioration of soil quality and development of active rills on-site and siltation of reservoirs off-site [17]. On-going severe soil erosion and land degradation has made large part of the watershed unsuitable for crop production, thereby decreasing food security. Despite the severity of soil erosion and its consequence on agricultural productivity and the environments in the area, especially in Alage watershed, there have been less systematic studies of soil erosion rates and its relation to land use land cover change.

Digital elevation model (DEM) along with remote sensing data and Geographical Information System (GIS) can be successfully

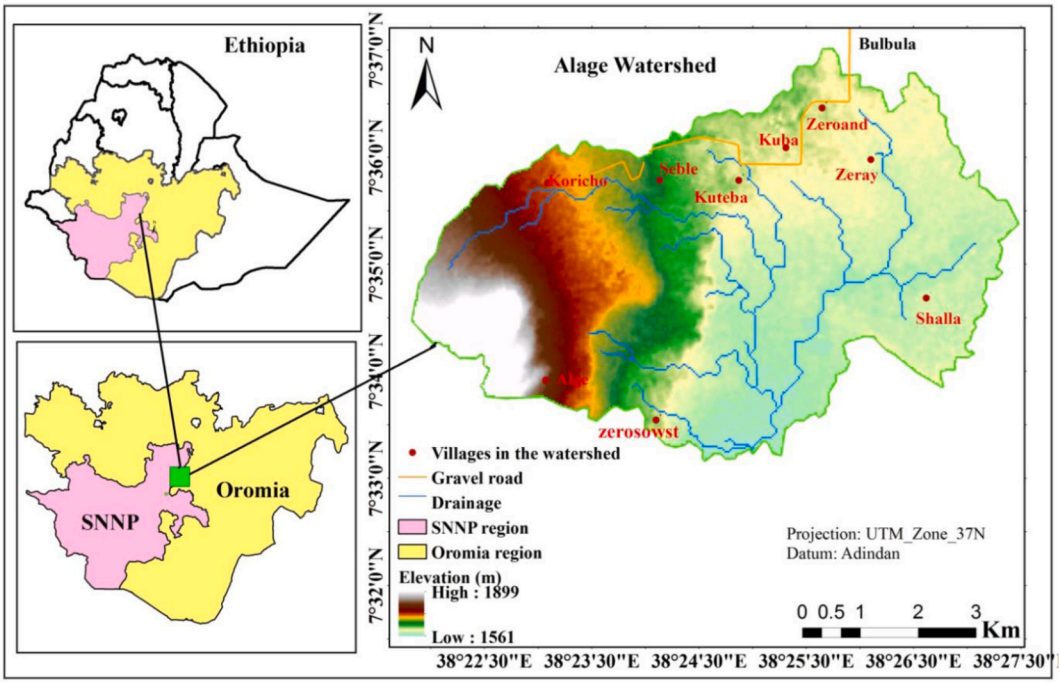

Fig. 1. Study area (Alage watershed) in between Oromia and Southern Nations Nationalities and Peoples (SNNP) regions, Ethiopia.

applied to enable rapid as well as detailed assessment of soil erosion hazards at large watershed scale [36–38]. Assessment and mapping of soil erosion rates in a watershed is important for the identification of critical hotspot areas for a targeted implementation of appropriate land management and rehabilitation measures [26,39].

Generating accurate environmental risk maps (e.g. landslide, soil erosion, flood, pest and diseases) in GIS environment is crucial to locate areas with high social and environmental risks. This is essential to develop adequate and targeted risk prevention strategies in advance. While Remote Sensing has proved to be a useful, inexpensive and time effective tool in soil erosion risk mapping at large scale, the method is less adopted for mapping soil erosion risk within the large watershed to help in designing of appropriate land management interventions and formulate land use policy in the study area. Therefore, this study is aimed at a) assessment of past and current soil erosion rates and trends for Alage watershed, b) mapping soil erosion hotspot areas and modelling the spatial and temporal trends of soil erosion, c) to evaluate the relation between land use land cover change and soil erosion rates during the different period in the watershed.

2. Materials and methods

2.1. Study area

The study was conducted in Alage watershed located in the central Rift Valley of Ethiopia, which is part of The East African Rift system [40]. Geographically, the studied watershed lies between 38°20′0" - 38°27′30″ E and 7°30′0" - 7°37′30″N (Fig. 1). The watershed has an area coverage of 43.5 km^2, and with elevation ranging from 1561 to 1899 m a.s.l. Topography is rugged varying from valley bottom to hills (Fig. 1). Climate of the study area is characterized by semi-arid type with a long-term average annual rainfall depth estimated at 708 mm and air temperature of 20.1 °C (Fig. 2). The rainfall is strongly seasonal and with significant spatial and temporal variability inducing frequent droughts [40]. The major soil types in the watershed are Fluvisols in the valley bottom and Leptosols on the hillslopes and escarpments. The dominant land use types are cropland (annual crop in rain-fed and irrigated crop production systems), bare land with no protective vegetation cover on slopes, and bush/shrub land. Due to rapid deforestation in response to expansion of cropland and heavy dependency on biomass energy, the areal coverage of forest land is very limited in the watershed.

The farming system is characterized as crop and livestock-based mixed farming. Croplands are tilled by both traditional ard plough (*maresha*) pulled by a pair of oxen and a few farmers till their land with tillage machinery. Tillage frequency varies from 1 to 4 times per season in response to available draft power and crop types [41]. The dominant crop and vegetables grown in the Alage watershed include: Maize (*Zea mays* L.), Haricot beans (*Phaseolus vulgaris* L.), Onion (*Allium cepa* L.), Pepper (*Capsicum annuum* L.), Tomato (*Solanum lycopersicum* L.), Papaya (*Carica papaya* L.), Banana (*Musa acuminate* Colla) and Mango (*Mangifera indica* L.) and some of these crops require supplementary irrigation for successful completion of their growth cycle.

2.2. Methods of data collection

To estimate the average annual soil loss rate of Alage watershed using the Revised Universal Soil Loss Equation (RUSLE), spatial and temporal datasets related to factors of the RUSLE were calculated (Fig. 3). These include multi-temporal satellite images (i.e. 1984, 2000 and 2016) years for land use land cover analysis. Long-term rainfall data acquired from the three measuring stations of the National Meteorological Agency is used to calculate R-factor (Fig. 2). Digital Elevation Model (DEM) at 30 m × 30 m spatial resolution

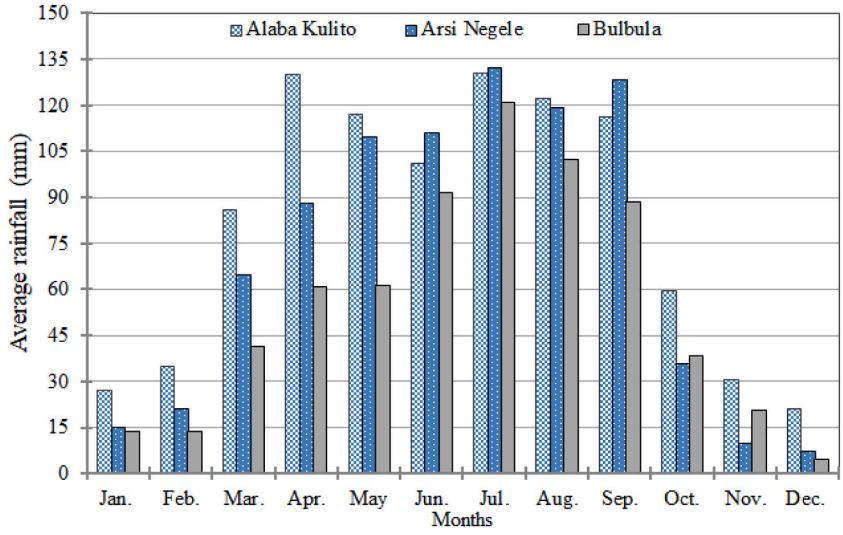

Fig. 2. Long-term (1998–2015) average monthly rainfall depth (mm). Rainfall data provided by the National Meteorological Agency (NMA) of Ethiopia.

is used to calculate topographic factors: slope length (L) and slope steepness (S). Spatially distributed soil samples which were collected for irrigation development, environmental and social impact assessment is used to determine the spatial soil erodibility (K-factor) values. The soil conservation practice factor is determined from the sub-factors such as contour tillage ($P_{cont.}$) and implemented soil and water conservation (SWC) measures. The P sub-factor due to tillage for cropland (i.e. $P_{cont.}$) was determined from land use land cover map and slope gradients based on [18,42]. SWC measures implemented in the watershed were also surveyed to determine (P_{swc} sub-factor). An extensive participatory field survey was conducted to record the different soil and SWC measures in the watershed and their corresponding P values are obtained based on literatures. The overall *P*-factor was calculated as a product of the sub-factors *P*-factor = $P_{cont} \times P_{SWC}$ [33,42]. Overall, integrated secondary and primary data sources were collected and used to calculate factors of the RUSLE, determine average annual soil loss values and mapping of soil erosion hotspot areas in the watershed (Fig. 3).

2.2.1. Land use land cover classification

Rainfall-runoff production, soil erosion and primary production processes taking place within a watershed strongly depends on the land use land cover types [22,43,44]. This study applied a supervised land use land cover classification system using maximum likelihood algorithm as proposed by Ref. [45]. We used ERDAS imagine 2014 to detect each of the land use land cover classes and changes during the three periods i.e. 1984, 2000 and 2016. Major land use land cover classes are identified based on the approach developed by Ref. [46]. These time period i.e. 1984, 2000 and 2016 were selected as the studied watershed experienced major land use land cover changes during these periods due to drought, increased human settlement, expansion of cropland area both in rain-fed and irrigated production systems [40,47]. Deforestation of afromontane forest, woodland and bush/shrub lands become rampant following the establishment of Alage Agricultural Technical Vocational Education and Technology (ATVET) College in 2002.

Data of land use types were collected from field ground control points (GCP) and Google earth image to validate the results of land use land cover classification using a confusion matrix (error matrix). This is conducted using Arc GIS 10.4. The overall accuracy was computed by dividing correctly classified pixels by the total number of pixels considered. Based on this, the accuracy for all land use land cover types classified during the periods of 1984, 2000, and 2016 were evaluated.

2.2.2. Determination of factors of the RUSLE

The RUSLE model is used to compute long-term average annual soil loss rate due to sheet and rill erosion [18,42,48]. It is developed as an empirical equation (model) representing the main factors controlling soil erosion processes, namely climate (rainfall erosivity), soil characteristics (soil erodibility), topography (slope length and slope steepness), cropping and cover-management and conservation

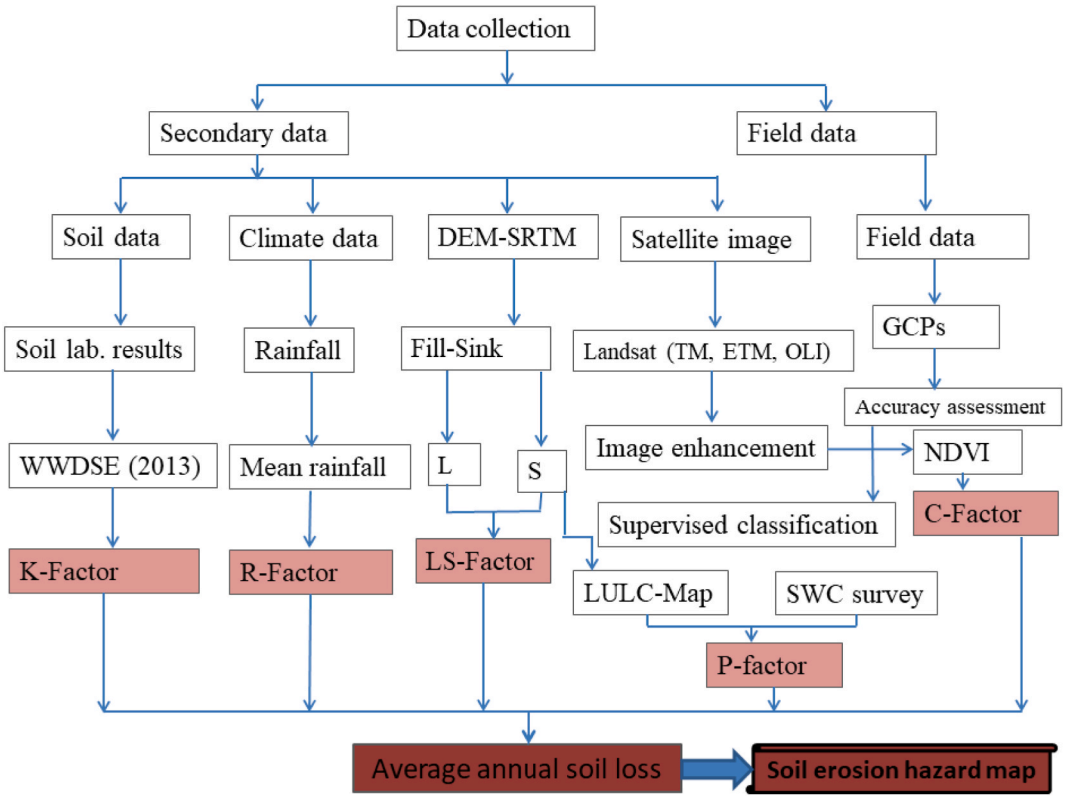

Fig. 3. Flow chart illustrating data collection and determination of factors of the RUSLE, estimation of the spatially distributed average long-term annual soil loss rate using RUSLE and erosion hazard mapping.

practice factors [18]. In this study we employed this model because it was realized from field observations that gully erosion and landslides are less common rather sheet and rill erosions are the most dominant forms of soil erosion in the study area. The RUSLE model is expressed in [Eq. (1)] [18];:

$$A = R * K * L * S * C * P \quad (1)$$

Where, A is the computed long-term average annual soil loss rate (ton ha^{-1} yr^{-1}); R is the rainfall erosivity factor (MJ mm ha^{-1} h^{-1} yr^{-1}); K is the soil erodibility factor (ton hr MJ^{-1} h mm^{-1}); LS is a combined slope length and steepness factor, C is the cropping and cover-management factor, and P is the erosion control or conservation practice factor [18]. These factors (LS, C and P) are all dimensionless. A raster map of the entire watershed (30 m × 30 m resolution) was developed for each of the factor of the RUSLE. This allowed for an overlay analysis of these raster layers in the ArcGIS environment to estimate spatially distributed long-term average annual soil loss rates during the different periods. The overlay analysis generated soil erosion pattern map in the watershed and identified soil erosion hotspot areas to be used for soil and water conservation interventions targeting at these critical locations in the watershed.

2.3. Rainfall erosivity (R) factor

Determination of the rainfall erosivity factor requires a long-term rainfall data especially rainfall intensity of an area [49]. However, rainfall intensity data is not available for most of the arid and semi-arid areas of developing countries. This is due to a limited capacity to measure rainfall intensity and also to the fact that rainfall intensity is highly variable in space and time in these environments. Therefore, the mean annual rainfall depth is used to calculate rainfall erosivity values based on an already established empirical relation between mean annual rainfall and erosivity for Ethiopia [Eq. (2)]; [50]. The rainfall data obtained from the three nearby meteorological stations were used (Table 1).

$$R = -8.12 + (0.562 \text{ x } P) \quad (2)$$

Where, R is rainfall erosivity value in MJ mm $ha^{-1}hr^{-1}yr^{-1}$, P is spatial distributed 17 years (1998–2015) mean annual rainfall depth in mm from the three stations (Table 1). The locations of the stations and the corresponding mean annual rainfall depth values were imported into ArcGIS 10.4 as point vector data. Then, an Inverse Distance Weighting (IDW) interpolation method was applied to create rainfall erosivity map of the entire watershed (Fig. 4A).

2.4. Soil erodibility (K) factor

Soil erodibility (K) factor is calculated based on a method proposed by Ref. [18]. The method [Eq. (3)] is based on soil properties and soil profile characteristics such as particle size distribution, organic matter content, soil structural code and profile permeability. For soils with silt fraction lower than 70% of the soil separate, soil erodibility can be calculated using [Eq. (3)]. Soil samples collected from the study area contain silt fraction of less than 70% and hence the proposed equation is appropriate [18,33,42].

$$K = \left[2.1 * 10^{-4} (12 - OM) M^{1.14} + 3.25(S - 2) + 2.5(P - 3)\right] / 100 \quad (3)$$

Where: OM is the percentage soil organic matter content, *M* is particle size parameter and is given by *M* = (%Silt + %Very Fine Sand) * (100 - %Clay), *S* is soil structural code, and *P* is the soil profile permeability rating were obtained using a combination of field observation and default values were considered for *S* and *P*. Based on the 23 soil samples collected from the entire watershed (Table 2), soil erodibility factor was estimated using IDW interpolation technique to produce spatial soil erodibility map for the entire watershed (Fig. 4B).

2.5. Slope length and steepness factor (LS)

The slope length and slope steepness factors are commonly combined in a single LS-factor or topographic factor. Slope length factor (L) is derived based on [18,51] and varies with slope length and slope length exponent (m) as given in [Eq. (4)]:

$$L = \lambda / (22.13) \quad (4)$$

Where, λ=slope length or distance of an overland flow measured in (m) and m is slope length exponent that depends on site slope gradient (**θ**) and rill to inter-rill ratio and calculated based on [Eq. (5), Eq. (6)]; [51].

Table 1
Mean annual precipitation (1998–2015) and rainfall erosivity values of the three rainfall stations.

RF stations	Latitude	Longitude	Elevation (m)	Mean annual RF (mm)	R-Factor (MJ mm $ha^{-1}hr^{-1}yr^{-1}$)
Alaba Kulito	7.31	38.094	1772.00	921.2	509.6
Arsinegele	7.36	38.66	1913	793.6	438.0
Bulbula	7.72	38.65	1606	620.8	340.8

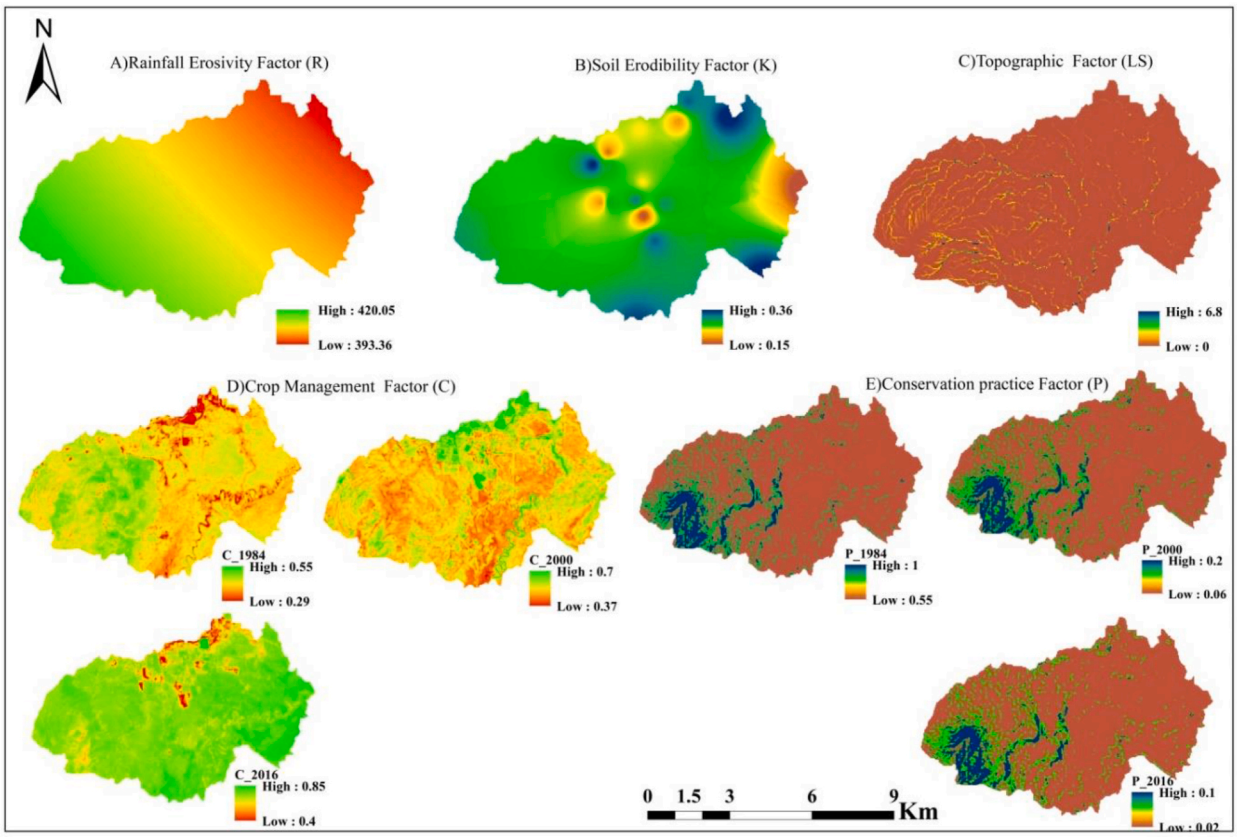

Fig. 4. Illustration of the spatial distribution of the factors of the RUSLE. The cover management (*C*-factor) and Conservation practice (*P*-factor, determined for the period of 1984, 2000 and 2016.

Table 2
Estimated K- factor values of the soil collected from the watershed.

Textural class	Soil Structural code	Soil Permeability	OM (%)	*M*	K –factor (MJ mm h^{-1} ha^{-1} $year^{-1}$)
Sandy clay loam	4	2	3.00	3600.03	0.30
Sandy loam	4	2	2.75	4514.14	0.32
Silt clay loam	3	5	5.03	3833.75	0.26
Clay loam	3	4	4.87	4949.35	0.30
Clay loam	3	4	3.28	4939.59	0.35
Loam	2	3	3.27	3503.51	0.20
Silt clay loam'	3	5	2.45	3840.01	0.33
Clay loam	3	4	3.74	5251.47	0.36
Clay loam	3	4	4.78	4245.98	0.26
Loam	2	3	3.37	4004.62	0.23
Loam	2	3	3.42	5952.98	0.36
Loam	2	3	6.14	7063.66	0.30
Silt loam	3	4	4.94	5769.16	0.32
Silt loam	3	4	1.51	3896.03	0.31
Clay loam	3	4	3.06	4489.72	0.33
Silt clay	4	6	3.38	3579.43	0.34
Loam	2	3	4.69	4651.24	0.23
Silt loam	3	4	2.20	4489.00	0.33
Sandy loam	4	2	2.41	4173.16	0.31
Silt loam	3	4	4.16	5937.83	0.36
Loam	2	3	2.19	2460.31	0.15
Sandy loam	4	2	1.98	2918.16	0.23
Silt clay loam	4	5	2.34	3540.25	0.34

$$m = \beta/(1+\beta) \tag{5}$$

$$\beta = (\sin\theta / 0.0896)/(3 * \sin(\theta)(0.8+0.56) \tag{6}$$

Since slope gradient of the watershed exceeds 25% and varies over a wide range, a general equation proposed for such area is used in each pixel as shown in [Eq. (7)] [52];:

$$S = -1.5 + \frac{17}{\left(1 + e^{(2.3-6.1*sin\ \Theta)}\right)} \tag{7}$$

Where, S is the slope steepness factor, and $\boldsymbol{\theta}$ is angle of the slope of a pixel in degrees. Summarizing equations (4)–(7) the LS factor for the watershed (Fig. 4C) was computed using Raster calculator in arc GIS10.4 as indicated in [Eq. (8)]:

$$LS = L * S \tag{8}$$

2.6. Cover-management (C) factor

The C factor reveals the effects of cropping and cover management factor. This factor takes into account the effects of vegetation canopy and ground covers in reducing soil erosion rate [18]. The raw Landsat imageries from the year 1984, 2000 and 2016 are converted to reflectance and NDVI. This is computed by utilizing red and near-infrared bands. A recent method for calculating cropping and cover management (C) factor [53] for the RUSLE based on NDVI for tropical climate [Eq. (9)] is applied. The values of C factor (Fig. 4D) can vary from 0 for soils with protective cover to 1 for finely tilled bare surfaces that produce much runoff making it more susceptible to rill erosion.

$$C = (-NDVI + 1)/2 \tag{9}$$

2.7. Support practice factor (P)

The *P*-factor values were assigned to a pixel considering contour tillage, slope gradients ($P_{cont.}$) and local soil and water conservation (SWC) practices (P_{SWC}). Thus a contour ploughing and slope gradients for calculating (P_{cont}); see Ref. [18] sub-factor was considered for the period 1984. Contour ploughing (P_{cont}) sub-factor and terracing (P_{SWC}) were considered for the period 2000 and combination of strip-cropping, contour ploughing and terracing for the period 2016. The reclassified slope was edited by adding a new field of *P*-values under the edit menu in Arc GIS 10.4 at the attribute view before *P*-factor was produced (Table 3). Finally, the theme was converted from vector form to grid form with the cell size of 30 m spatial resolution to produce P factor layer) of the entire watershed (Fig. 4E).

3. Results and discussion

3.1. Factors of RUSLE

The calculated rainfall-runoff erosivity (R-factor) values ranges from 340.8 at Bulbula station to 509.6 MJ mm $ha^{-1}hr^{-1}$ yr^{-1} at Alaba Kulito station (Table 1). The rainfall erosivity values estimated from the produced erosivity map ranged from 393 to 420 MJ mm $ha^{-1}hr^{-1}yr^{-1}$ (Fig. 4A). The highest rainfall erosivity value is observed in the Western part of Alage watershed due to the combination of higher elevation induced large drop size [54], relatively higher rainfall and steep slope. The rainfall erosivity gradually decreases from western to the eastern part of the watershed. Ref. [55] clearly indicated that the western part of the Rift Valley require soil conservation due to high rainfall compared to the eastern part and the rift floor. Similarly, in Koga watershed where the long-term average annual rainfall is larger than 1500 mm, reported rainfall erosivity values ranged from 810 to 1030 MJ mm $ha^{-1}hr^{-1}yr^{-1}$ [48]. In line with our results [56], also reported rainfall erosivity value ranging from 530 to 643 MJ mm $ha^{-1}hr^{-1}yr^{-1}$ for Awasas Lake catchment within the Rift Valley system where average annual rainfall ranged from 957 to 1159 mm.

Soils of the study area can be categorised into seven soil textural classes based on the relative proportion of sand, silt and clay (Table 2). The calculated soil erodibility (K-factor) values ranged from 0.15 to 0.36 MJ mm h^{-1} ha^{-1} yr^{-1}. These values are by far larger than those values (0.009–0.04) reported for semi-arid Ethiopia highlands due to the absence of surface rock fragment cover in Alage watershed [33,42]. Such lower soil erodibility factor values for the semi-arid hillslopes are attributed to significant surface rock

Table 3
Support practice factor value for contouring, strip cropping and terracing based on slope gradient of the studied watershed.

Slope (%)	Contouring	Strip cropping	Terracing
0–7	0.55	0.27	0.1
7–11.3	0.6	0.3	0.12
11.3–17.6	0.8	0.4	0.16
17.6–26.8	0.9	0.45	0.18
26.8>	1	0.5	0.2

fragment cover which reduced soil erodibility by intercepting rain drop impact and infiltration. For Omo Gebi River basin of the south western Ethiopia, calculated K-factor values ranged from 0.33 to 0.62 [26]. The high K-factor values for Alage watershed in the Rift Valley is associated to soils having low permeability, due to higher clay content of the soils of valley bottom (Fig. 4B). Based on soil color, [32] reported soil erodibility factor values of the soils in the Rift Valley region ranging from 0.15 to black soils to 0.3 to yellow soils. On average, large areas of the entire watershed fall into moderate to high soil erodibility values indicating the vulnerability of the soils in the watershed to erosion processes.

The spatial pattern and variation of the combined LS-factor values for the studied watershed is presented in (Fig. 4C). The topographic factor values range from 0 to 6.8. It can be seen from the LS-map that the lower LS-factor values are clearly observed along the valley bottom (rift floor) and flat areas of the watershed. Higher LS values are observed in the mountainous area with steep slope in the western highlands parts of the watershed. Variations of LS-factor values can be attributed to the complex rugged landforms of the watershed, higher LS values are clearly located in erosion affected areas of Alage watershed. In contrast to our results [57] reported that the combined slope length and slope steepness (LS) factor values ranging from 0 to 78.48 for Dijo watershed located in the Rift Valley basin with average value for the watershed being 0.56. Similarly, for a large watershed in India, Jharkhand state [58], reported the combined LS factor value ranging from 0 to 11.1.

The mean value of NDVI for the studied year 1984, 2000 and 2016 are 0.15, −0.08,-0.27 respectively, which indicates a progressively decreasing tends of protective vegetation cover in the area. The corresponding calculated *C*-factor values ranged from 0.29 to 0.55 in 1984, 0.37 to 0.70 in 2000 and from 0.40 to 0.85 in 2016 (Fig. 4D). The *C*-factor values are lower for very well vegetated part and high for finely tilled bare surfaces that produce high runoff and soil loss. The C-factor values are consistently increased from 1984 to 2016 indicating rapid land use land cover change and decreasing trends of vegetation cover. Increasing C-factor values from 1984 to 2016 is clear indication of increasing proportion of bare and cropland areas during the period. In the semi-arid Tigray cover management factor values were reported to be 0.004 for forest and exclosures, 0.07 for teff fields, 0.21 for wheat fields and 0.42 for degraded rangeland using experimental runoff plots [33].

In line with our results [50], reported C-factor values that range from 0.10 to 0.25 for arable land with different crop types based on plot data. Similar to our results, [26] indicated an increasing trends of the C-factor values for the different land use types during the period 1988 to 2018 for Winike watershed of Omo Gibe Basin, Ethiopia. The values ranging from 0.15 to 0.21 for built up area, 0.21 to 0.27 for bare land, 0.012 to 0.042 for bush/shrub land, 0.012 to 0.05 for grazing land and 0.11 to 0.26 for cultivated land were reported. The C-factor values strongly depend on land use types and vegetation cover providing soil protection against direct rainfall and runoff erosivity [26,33,42,57].

The support practice *P*-factor values generally ranges from 0 to 1. Lower *P*-factor values indicate effective soil and water conservation practices. During the field survey, it has been observed that the entire watershed is not treated with structural soil and water conservation measures. The calculate *P*-factor values of Alage watershed ranged from 0.55 to 1 in 1984, 0.06 to 0.20 in 2000 and from 0.02 to 0.2 in 2016 (Fig. 4E). Implemented soil and water conservation measures are increasing in type and area coverage from 1984 to 2016 (Table 3) and hence the resulting *P*-factor values decreased from 1984 to 2016 (Table 3). In line with this, based on plot scale study [42], determined and reported conservation practice factor values ranging from 0.03 to 0.74 for the runoff plots treated with different soil and water conservation measures on rangeland and cropland sites. In Awassa catchment where soil and water conservation measures are less common [56] estimated conservation practice factor ranging from 0.8 to 0.9.

3.2. Estimated soil erosion rate

The result showed that the potential current average annual soil loss rate from Alage watershed ranges from 0 at valley bottom to 106 ton ha^{-1} yr^{-1}on steep slope and mountainous part of the watershed. The overall current average annual soil loss rate for the watershed is 38 ton ha^{-1} yr^{-1} which is above the tolerable soil loss rates of 2–18 ton ha^{-1} yr^{-1} proposed for Ethiopian conditions [50] and is within the range of reported soil loss values for other environments (Table 4). Low soil erosion risky areas correspond to river valleys or gentle slopes areas whereas high erosion risk or hotspot areas are situated along the steeper slope banks of tributaries

Table 4
Comparison of reported soil loss rates to reported long-term average, annual and seasonal rates. Soil loss value in parenthesis is an average of measured or estimated soil loss rate. NA is not available.

Country	Land use type	Climatic region	Measurement scale	Slope gradient (%)	Soil loss (ton $ha^{-1}yr^{-1}$)	Sources
Ethiopia	Multiple	Tepid moist	Watershed	0 - >30	0–716 (42)	[48]
Ethiopia	Rangeland	Semi-arid	Plot (600–630 m^2)	5–16	28.6–50 (38.1)	[59]
Ethiopia	Multiple	Semi-arid	Watershed	0–48	0–106 (38)	This study
Ethiopia	Cropland	Semi-arid	Plot (770–1000 m^2)	5–16	4.6–15.5 (9.8)	[59]
Ethiopia	Multiple	Semi-arid	Plot (300–3900 m^2)	5–50	3.5–17.4 (9.9)	[33]
Ethiopia	Cropland	Sub-humid	Watershed	0–89.9	10.02–43.48 (NA)	[26]
Morocco	Multiple	Arid and Semi-arid	Argana corridor	0 - >26.81	0–160.3 (47.52)	[60]
India	Multiple	NA	Watershed	0–90	0.005–170 (13.21)	[58]
Ehiopia	Multiple	Humid tropics	Sub basin	0–269	0–932.6 (83.)	[29]
Ethiopia	Multiple	NA	Watershed	0–40	0–202 (NA)	[56]
Ethiopia	Multiple	Semi-arid	Watershed	0 - >30	4.4–37.5 (24.2)	[31]
Ethiopia	Multiple	Humid tropics	Watershed	0–100	0–897 (25)	[61]
Ethiopia	Multiple	Sub-humid	Sub-basin	0–42.6	0–958 (64)	[11]

(Fig. 5). This result is in line with the results of soil erosion risk assessment study who indicated an average annual soil loss rate in central Rift Valley of Ethiopia to be 41 ton $ha^{-1}yr^{-1}$ [32]. Similarly, with the application of the RUSLE the average annual soil erosion rate for Koga watershed located in the north-western part of Ethiopia is estimated at 42 ton ha^{-1} yr^{-1} with a range of soil loss ranging from 0 to 716 ton ha^{-1} yr^{-1} [48]. The highest soil loss rate is attributed to land use change on slope followed by an intensive farming in response to population growth and also near river channels due to concentrated flow. Based on analysis of the spatial and temporal variation of rainfall and rainfall erosivity in the Rift Valley system, Ethiopia [55] reported decreasing trends in rainfall erosivity from 2000 to 2010. They also emphasized that the increasing rate of resources degradation such as soil erosion in Rift Valley is mainly attributed to human impact through land use land cover change.

The largest portion of the studied watershed covering 42.83 km^2 (98.5%) fall within low and moderate soil erosion risk classes due to its gentle slope gradients (Fig. 5). The other soil erosion risk classes, high, very high and extreme erosion risk classes accounted for 0.52 km^2 (1.16%), 0.13 km^2 (0.3%) and 0.02 km^2 (0.04%) of the watershed respectively. The areal coverage of each soil erosion risk classes has the same magnitude with previous study reported by Ref. [56]. Using USLE and GIS for Awassa catchment, they indicated that soil erosion risk classes as low 94.8%, moderate 2.68%, high 1.62%, very high 0.4% and extreme 0.02%. These high to extreme soil erosion risky areas particularly from cultivated land on steep slope has resulted in a continuous reduction of crop yields and are the major sources of sediment for siltation of irrigation dam located in Alage watershed. In contrast 95.2% of Modjo watershed fall under moderate to severe soil erosion classes with soil loss values ranging from 14.7 to 37.5 ton ha^{-1} yr^{-1} with the application of Soil and Water Assessment Tool (SWAT) model [31]. Based on their study at Anger River sub-basin of the western Ethiopia [29], reported that 43.6% of the sub-basin is classified as very severe erosion classes with average annual soil loss being 83.7 ton ha^{-1} yr^{-1}.

High soil erosion rates were also observed on the landform having steep and very steep slope gradient, structural valley and structural hills areas that are associated with high drainage density [48,62]. The low soil erosion risky areas are mostly located along the river valleys or gentle slope areas, where the low slope gradients allow accumulation of materials transported by water or gravity from the hillslopes. The soils in these area are also deeper, contain more organic matter and has better permeability and water holding capacity than the soils on the hillslopes of the watershed which are low in organic matter content and shallow depth. The spatial locations of the hotspots (Fig. 5) revealed that the potential for soil loss is typically higher on a longer, steep slope and banks of gullies and tributaries and also cover very small part of the watershed. These areas can be targeted for conservation planning and the implementation of appropriate land use system and land rehabilitation measures to reduce soil erosion to a tolerable level.

Reported range and average annual soil loss rate are within the range of soil loss values reported for semi-arid environments (Table 4). In line with our results [31], reported that due to land use land cover change between 1973 and 2007 in Modjo watershed, central Ethiopia, surface runoff and sediment yield increased by 14.2% and 37% respectively. Ref. [11] also reported that soil erosion rate increased from 53.2 ton ha^{-1} yr^{-1} in 1986 to 64 ton ha^{-1} yr^{-1} in 2020 for Muger sub-basin of the upper Blue Nile basin and attributed to the increased proportion of the basin exposed to soil erosion.

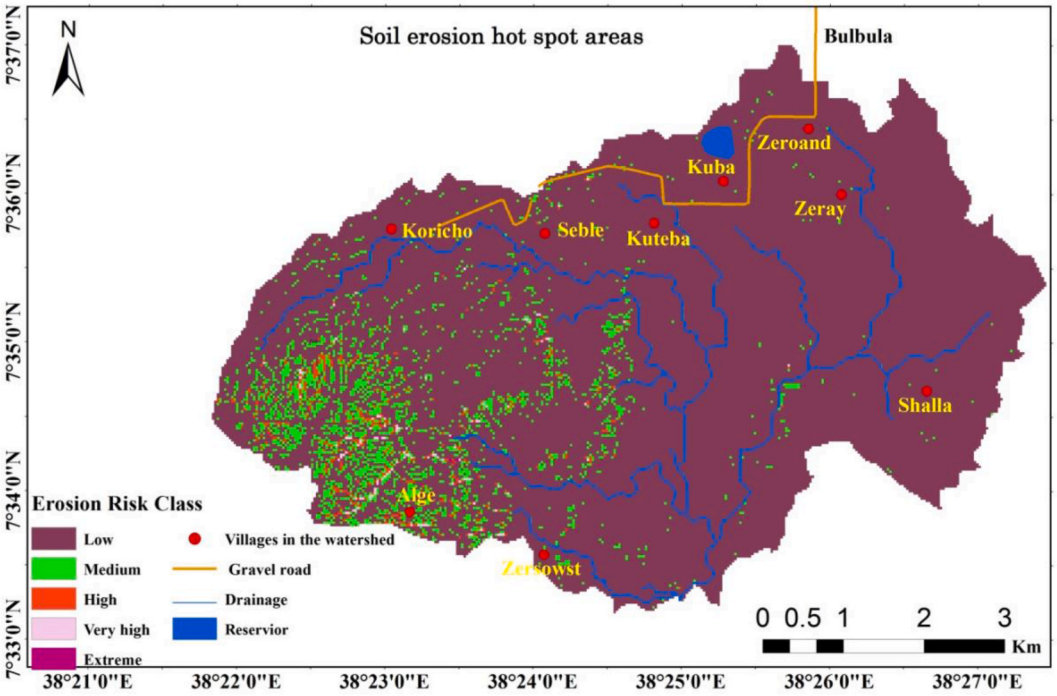

Fig. 5. Soil erosion risk map of the Alage watershed showing spatial distribution of different soil erosion classes.

3.3. Land use land cover change analysis

The results of land use land cover classification indicated eight land use classes including rainfed cropland, forest land, grassland, bush/shrub land, irrigated cropland, water bodies, bare land and settlement areas for each of the period considered in 1984, 2000 and 2016 (Fig. 6). The spatial distribution of land use land cover categories of the study area during the period of 1984, 2000 and 2016 revealed that coverage of bare land, cultivated land, and settlement area increased. Bush/shrub land, forest, grassland, irrigated cropland and water body coverage decreased during those periods (Table 5; Fig. 6). In a line of this [26] reported that coverage of cropland, bare land, built up areas and woodland increases while the coverage of shrub land, forest, grazing, and water bodies decreased over a period of 1988–2018 for Omo Gibe basin, Ethiopia. Similarly, in central Gojam [24] reported a significant land use land cover change in response to population growth and expansion of agricultural land. It is also indicated that such land use land cover change leading to decreased proportion of forest and woodland is among the major causes to the observed soil erosion by water [7,24,26,27,55].

This change in land use land cover i.e. increasing proportion of cropland, bare land and built up area contributed to the increasing soil erosion rates during the period 1984 to 2016. In the same line significant association among land use land cover change, climate and geomorphological conditions to soil erosion has been reported [26,32,58].

Land use land cover classification results of the 1984 and spatial distribution of land use types is indicated (Fig. 6A). Moreover, the areal and percent coverage of each land use land cover type presented in Table 5 indicated that the dominant land use in 1984 is cropland while bush/shrub land also cover an equivalent proportion. This indicated that human impacts such as deforestation and land use conversion to cropland is already high in the watershed before 1984. The proportion of cropland, bare land and built up area remarkably increased during 2000 and 2016 (Table 5) compared to the coverage at base year (1984). Similar studies in Ethiopia reported an increasing proportion of cropland [25,63–66] and attributed this change to increased human population pressure and the need to expand agricultural land use system through deforestation and land use conversion (Fig. 6B and C). Our results showed that the area coverage of cropland increased from 36.3% in 1984 to 53.6% in 2016. In line with this [25] reported that cropland area increased from 85.4% in 1986 to 93.3% in 2017 for Dega Damot district located in the North-western highlands of Ethiopia. Analysis of land use land cover change for Gibe valley of the south-western Ethiopia indicated that drought, migration, change in settlement and land use policy as major driver of the observed changes over the period of 1957–1993 [66].

In contrast to the observed trends of increasing areal coverage of cropland and bare land [45] reported decreasing proportion of cultivated land by 0.02% (323.4 ha) and bush/shrub land by 3.41% (515.44 ha) for Yezat watershed West Gojam Amhara region, Ethiopia. They attributed such trends to an integrated watershed development program and increased vegetation cover in the watershed. Our results also reveals overall an accuracy of the classifications found to be 83%, 85% and 90% was achieved with a Kappa

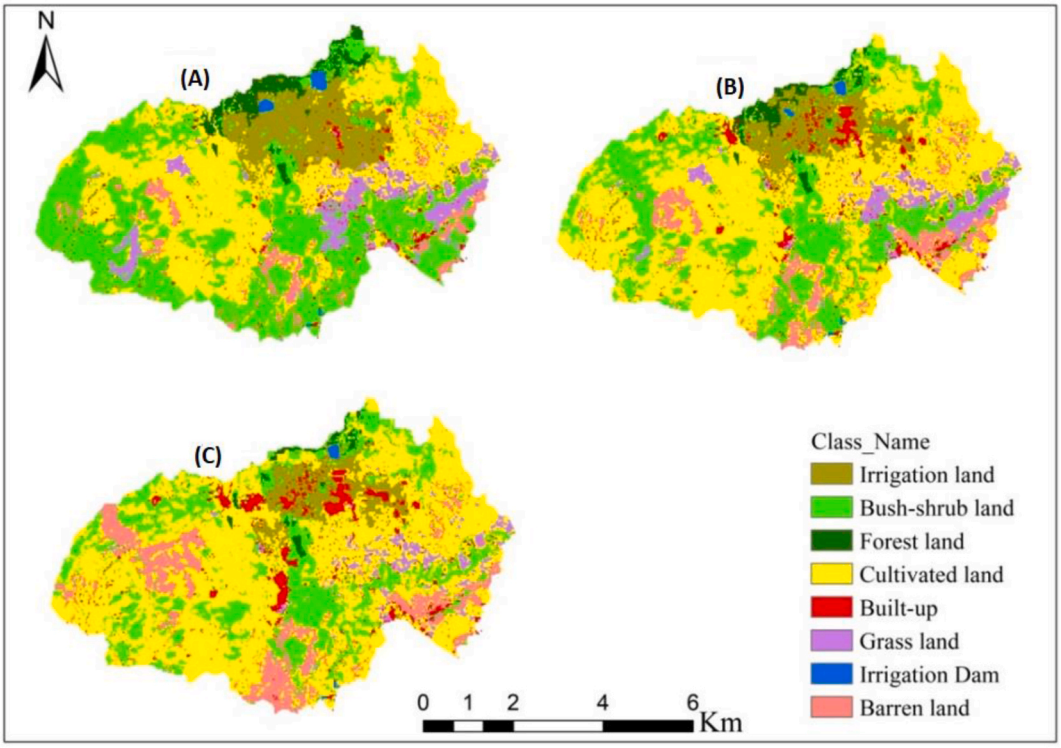

Fig. 6. Land use land cover types for Alage watershed during periods (A)1984, (B) 2000, and (C) 2016.

Table 5
Comparison of the areas of land-use/land-covers during 1984, 2000 and 2016.

Land-use classes	1984		2000		2016	
	Area (ha)	%	Area	%	Area (ha)	%
Bush/shrub land	1509.45	34.7	1055.7	24.27	834.3	19.18
Cropland	1576.87	36.25	2126.7	48.89	2332.03	53.61
Grass land	306.24	7.04	233.59	5.37	157.91	3.63
Irrigated cropland	475.89	10.94	354.96	8.16	273.18	6.28
Bare land	230.1	5.29	324.51	7.46	488.07	11.22
Forest land	150.08	3.45	92.66	2.13	50.03	1.15
Water body	22.62	0.52	11.31	0.26	8.7	0.2
Built up	82.65	1.9	153.56	3.53	209.24	4.81

coefficient of 0.79, 0.81 and 0.87 for the three Scenes (Landsat TM 1984, ETM^{+}2000 and OLI 2016), respectively. Increased area coverage of cropland, bare land and settlement area in the Alage watershed comes from the conversion of bush/shrub land, grass land, irrigated cropland, forest land and water bodies with decreasing area coverage during the same period (Table 6). Decreased water body and irrigated cropland are related as a decreased in available water leads to decreased irrigated areas. Large scale commercial irrigation in the Rift Valley is started in 1970 [67] and leading to a decreased water quantity and quality due to siltation and water pollution [26,40].

3.4. Soil erosion trends and land use land cover change

Estimated soil erosion rates for Alage watershed ranged from 0 to 78.4 ton ha^{-1} yr^{-1} in 1984, from 0 to 97 ton ha^{-1} yr^{-1} in 2000 and from 0 to 106 ton ha^{-1} yr^{-1} in 2016 (Fig. 7). The overall soil loss ranges and average values showed an increasing trends from 1984 to 2016. The average soil loss rate for the watershed was 24.3 ton ha^{-1} yr^{-1} in 1984, 33.9 ton ha^{-1} yr^{-1} in 2000 and 38 ton ha^{-1} yr^{-1} in 2016. In line with our results [32], reported an increasing trends of soil erosion rate between 1973 and 2006 for the central Rift Valley region. Reported average rates were 31 ton ha^{-1} yr^{-1} in 1973 and increased to 56 ton ha^{-1} yr^{-1} in 2006 and attributed to degradation of vegetation resources due to increased deforestation than change in rainfall erosivity [55]. Similarly [58], reported that the range of soil erosion rate at watershed scale in India was 0.008–150 ton ha^{-1} yr^{-1}in 1988 and increased to 0.05–169.92 ton ha^{-1} yr^{-1} in 2004 with average rate slightly increasing from 12.11 ton ha^{-1} yr^{-1} to 13.21 ton ha^{-1} yr^{-1} during the same period. In the Omo Gibe Basin of the South-West Ethiopia, soil loss from cropland estimated at 10.02 ton ha^{-1} yr^{-1} in 1988 increased to 43.48 ton ha^{-1} yr^{-1} in 2018 [26]. They attributed this to the expansion of cultivated land on marginal hillslope with >34% slope gradients. Land use land cover change and rugged topography combined with inappropriate conservation practices are the most important drivers of the soil erosion in Alage Watershed.

The change from forest or grass land to cropland, bare land or settlement area reduced protective vegetation cover and expose the soil to direct rain drop and wind impact. Land use change followed by agricultural expansion is reported to be responsible for increase of soil erosion rate from 36.89 ton ha^{-1} yr^{-1} in 1986 to 48.05 ton ha^{-1} yr^{-1} in 2020 [68]. Increasing soil erosion rate is related to both the removal of protective vegetation cover and decreasing soil organic carbon content caused by tillage and oxidation. This further enhances soil susceptibility to erosion and depletion of soil nutrients and its water holding capacity.

The mean NDVI values during the year 1984, 2000 and 2016 were 0.15, −0.08, −0.27 respectively. This indicates that vegetation cover in the watershed is decreasing from 1984 to 2016 due to the observed land use conversion and increased human impact. Similarly, the average cover-management (*C*-factor) values were 0.55 in 1984, 0.7 in 2000 and 0.85 in 2016. This progressively increasing trend in C-factor values are an implication for temporal and spatial increasing trends of soil erosion rate in the entire watershed. In line with this [69] indicated assessment and mapping of land degradation and desertification using NDVI values in a semi-arid area of India. In response to increasing soil erosion in Alage watershed, soil and water conservation practices are increasing as shown by a decreasing conservation practice factor values from 1984 to 2016. However, conservation measures were implemented on a limited part of the watershed by individual farmers and could not halt or reduced soil loss rate at large watershed scale. Based on

Table 6
Land-cover classes and rates of change in the study area during 1984, 2000 and 2016.

Land-use classes	1984–2000		2000–20016		1984–2016	
	Area (ha)	%	Area (ha)	%	Area (ha)	%
Bush/shrub land	−453.75	−10.43	−221.4	−5.09	−675.15	−15.52
Cropland	549.83	12.64	205.33	4.72	755.16	17.36
Grass land	−72.65	−1.67	−75.68	−1.74	−148.33	−3.41
Irrigation land	−120.93	−2.78	−81.78	−1.88	−202.71	−4.66
Bare land	94.41	2.17	163.56	3.76	257.97	5.93
Forest land	−57.42	−1.32	−42.63	−0.98	−100.05	−2.3
Water body	−11.31	−0.26	−13.92	−0.06	−13.92	−0.32
Built-up	70.91	1.63	55.68	1.28	126.59	2.91

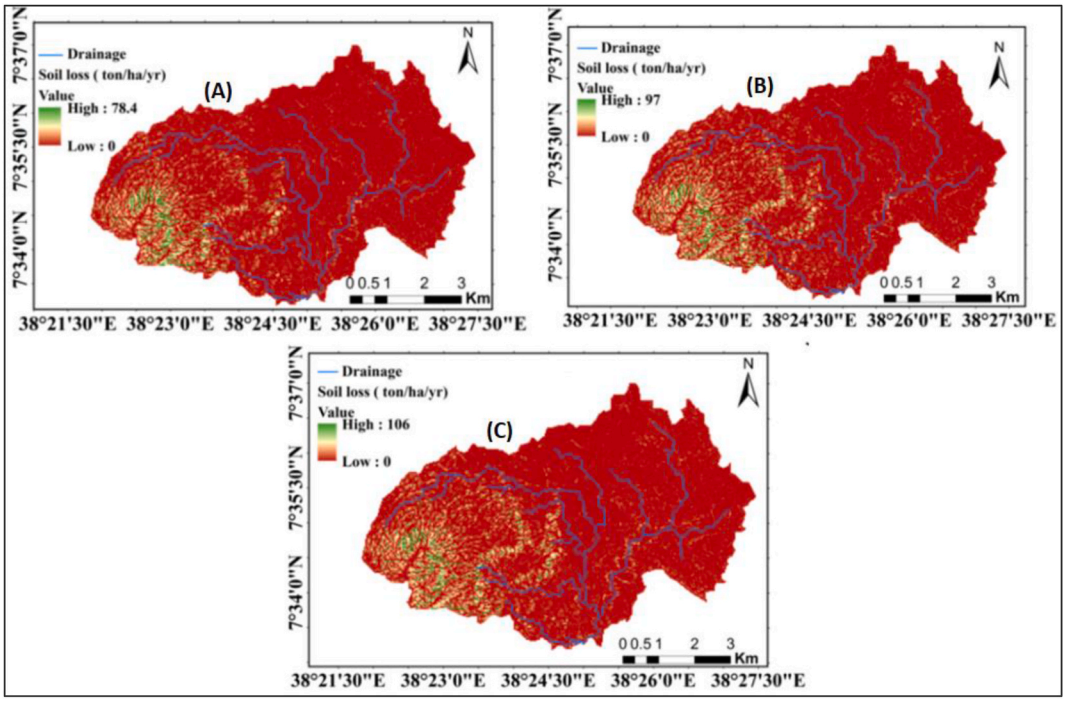

Fig. 7. Estimated spatial pattern of soil loss from the entire watershed showing minimum and maximum rates during the periods: (A) in 1984, (B) in 2000 and (C) in 2016.

their study to link land use land cover change and soil erosion rates [70], found close association among landscape characteristics such as aggregation index (AI), Shannon's diversity index (SHDI), largest patch index (LPI), patch cohesion index (COHESION) and contagion (CONTAG). These landscape characteristics accounted for 65% of the soil erosion and 74% of the sediment yield variation for the Upper Du River watershed of China.

4. Conclusions

Ethiopia being a developing and agrarian country it is very crucial and urgent to study the causes of land degradation to design and implement effective soil erosion and land degradation controlling mechanisms targeting at the hotspots. In most parts of Ethiopia, land degradation is manifested in the form of accelerated soil erosion. Alage watershed located in the Rift Valley areas is characterized by erosion susceptible arable lands and bare lands located on hillslopes. In this study a mixed approach of field investigation and adopted RUSLE modelling was used for soil erosion assessment during the periods 1984, 2000 and 2016. The RUSLE output indicates that average soil erosion rate has increased from 24.3 ton ha^{-1} yr^{-1} in 1984 to 38 ton ha^{-1} yr^{-1} in 2016. This increased in soil erosion rate is attributed to the observed rapid land use land cover change in particular to the increased proportion of cropland, bare land and built up areas at the expense of bush/shrub land, grassland and forest land in the middle and higher elevation of Alage watershed. Between the periods 1984 to 2016, significant land use land cover change has been observed leading to low values of the normalized difference vegetation index (NDVI) which has in turn resulted into accelerated soil erosion rate as protective natural vegetation coverage decreased. The proportion of crop land increased from 36.25% in 1984 to 53.61% in 2016 while bush/shrub land decreased from 34% in 1984 to 19.18% in 2016. Though large part of the watershed is classified as low to moderate soil erosion classes an average value of soil loss is still larger than the soil loss tolerance values of 2 ton ha^{-1} yr^{-1} to 18 tons ha^{-1} $yr^{-1}$for Ethiopia. The watershed area with high soil erosion i.e. hotspots require immediate soil and water conservation planning and implementation measures to reduce further soil loss and development of gully on those sites. Environmental rehabilitation through greening of degraded land using exclosures should be promoted to maintain or enhance shrub/bush land and natural protective soil cover.

Author contribution statement

Gebeyehu Taye: Conceived and designed the experiments; Performed the experiments; Analyzed and interpreted the data; Wrote the paper. Tesfaye Teklesilassie: Conceived and designed the experiments; Performed the experiments; Analyzed and interpreted the data; Wrote the paper. Daniel Teka: Contributed reagents, materials, analysis tools or data; Analyzed and interpreted the data. Henok Kassa: Analyzed and interpreted the data, wrote the paper.

Data availability statement

The data will be made available on request.

Funding statement

Research funding from Mekelle University is provided through The University recurrent budget for research. Recurrent budget alloted for the colleges and institutes of the university. This research is supported by Institute of Geoinformation and Earth Observation Science with ID: Recurrent IGoS 2016.

Declaration of competing interest

The authors declare that they have no known competing financial interests or personal relationships that could have appeared to influence the work reported in this paper.

Acknowledgement

We thank Mekelle University for providing research fund to Mr. Tesfaye Teklesilassie when he was conducting his master thesis field work in Alage watershed. We appreciate the project feasibility study of irrigation development, environmental and social impact assessment (WWDSE) for providing spatial soil data used for the determination of soil erodibility (K-factor) values. Farmers of the study area also deserve a special appreciation for their hospitality and facilitating the field work.

References

[1] D. Wuepper, P. Borrelli, R. Finger, Countries and the global rate of soil erosion, Nat. Sustain. 3 (2020) 51–55.
[2] Y. Ostovari, S. Ghorbani-Dashtaki, H.A. Bahrami, M. Naderi, A. Dematte, Soil loss prediction by an integrated system using RUSLE, GIS and remote sensing in semiarid region, Geoderma Regional 11 (2017) 28–36.
[3] P. Borrelli, D.A. Robinson, L.R. Fleischer, E. Lugato, C. Ballabio, C. Alewell, K. Meusburger, S. Modugno, B. Schütt, V. Ferro, V. Bagarello, K. Van Oost, K. Montanarella, P. Panagos, An assessment of the global impact of 21st century land use change on soil erosion, Nat. Commun. 8 (1) (2017) 1–13.
[4] G. Sterk, M. Riksen, D. Goossens, Dryland degradation by wind erosion and its control, Ann. Arid Zone 40 (3) (2021) 351–367.
[5] R. Lal, Soil erosion and conservation in west africa, in: D. Pimentel (Ed.), World Soil Erosion and Conservation, Cambridge University Press, Cambridge, 1993, pp. 7–26.
[6] M. Gharibreza, M. Zaman, P. Porto, E. Fulajtar, L. Parsaei, H. Eisaei, Assessment of deforestation impact on soil erosion in loess formation using 137Cs method (case study: golestan Province, Iran), Int. Soil and Water Conserv. Res. 8 (4) (2020) 393–405.
[7] J. Nyssen, J. Poesen, J. Moeyersons, J. Deckers, M. Haile, A. Lang, Human impact on the environment in the Ethiopian and Eritrean highlands—a state of the art, Earth Sci. Rev. 64 (3–4) (2004) 273–320.
[8] H. Hurni, Land degradation, famine, and land resource scenarios in Ethiopia, in: D. Pimentel (Ed.), World Soil Erosion and Conservation, Cambridge University Press, Cambridge, 1993, pp. 27–62.
[9] Z. Adimassu, S. Langan, R. Johnston, W. Mekuria, T. Amede, Impacts of soil and water conservation practices on crop yield, run-off, soil loss and nutrient loss in Ethiopia, review and synthesis, Environ. Manag. 59 (2017) 87–101.
[10] R. Lal, Soil erosion impact on agronomic productivity and environment quality, Crit. Rev. Plant Sci. 17 (4) (1998) 319–464.
[11] D.S. Teshome, M.B. Moisa, D.O. Gemeda, S. You, Effect of land use-land cover change on soil erosion and sediment yield in muger sub-basin, upper Blue Nile basin, Ethiopia, Land 11 (12) (2022) 2173.
[12] A. Aga, A. Melesse, B. Chane, Estimating the sediment flux and budget for a data limited Rift Valley lake in Ethiopia, Hydrology 6 (1) (2018) 1–22.
[13] N. Haregeweyn, J. Poesen, J. Nyssen, J. De Wit, M. Haile, G. Govers, J. Deckers, Reservoirs in Tigray (northern Ethiopia): characteristics and sediment deposition problems, Land Degrad. Dev. 17 (2) (2006) 211–230.
[14] M. Vanmaercke, A. Zenebe, J. Poesen, J. Nyssen, G. Verstraeten, J. Deckers, Sediment dynamics and the role of flash floods in sediment export from medium-sized catchments: a case study from the semi-arid tropical highlands in northern Ethiopia, J. Soils Sediments 10 (2010) 611–627.
[15] M.G. Kebedew, S.A. Tilahun, M.A. Belete, F.A. Zimale, T. Steenhuis, Sediment deposition (1940–2017) in a historically pristine lake in a rapidly developing tropical highland region in Ethiopia, Earth Surf. Process. Landforms 46 (8) (2021) 1521–1535.
[16] S. Issaka, M.A. Ashraf, Impact of soil erosion and degradation on water quality: a review, Geol. Ecol. Landsc. 1 (1) (2017) 1–11.
[17] T. Ayenew, Water management problems in the Ethiopian rift: challenges for development, J. Afr. Earth Sci. 48 (2007) 222–236.
[18] K. Renard, G. Foster, A. Weesies, K. Mccool, C. Yoder, Predicting soil erosion by water: a guide to conservation planning with the Revised Universal Soil Loss Equation (RUSLE), in: Agriculture Handbook, United States Department of Agriculture, Washington, 1997, pp. 1–404.
[19] R. Morgan, Soil Erosion and Conservation, third ed.s, Blackwell Science Ltd a Blackwell Publishing company, 2005, pp. 1–316.
[20] L. Stroosnijder, Measurement of erosion: is it possible? Catena 64 (2) (2005) 162–173.
[21] K. Ebabu, G. Taye, A. Tsunekawa, N. Haregeweyn, E. Adgo, M. Tsubo, A.A. Fenta, T.D. Meshesha, D. Sultan, D. Aklog, T. Admasu, B. van Wesemael, J. Poesen, Land use, management and climate effects on runoff and soil loss responses in the highlands of Ethiopia, J. Environ. Manag. 326 (2023), 116707.
[22] G. Taye, J. Poesen, B. Van Wesemael, M. Vanmaercke, D. Teka, T. Goosse, J. Deckers, W. Maetens, J. Nyssen, V. Hallet, N. Haregeweyn, Effects of land use, slope gradient, and soil and water conservation structures on runoff and soil loss in semi-arid northern Ethiopia, Phys. Geogr. 34 (3) (2013) 236–259.
[23] M. Haile, K. Herweg, B. Stillhardt, Sustainable Land Management –A New Approach to Soil and Water Conservation in Ethiopia, Switzerland Centre for Development and Environment (CDE) and NCCR North-South, Berne, 2006, pp. 1–304.
[24] H. Hurni, K. Tato, G. Zeleke, The implications of changes in population, land use, and land management for surface runoff in the upper Nile basin area of Ethiopia, Mt. Res. Dev. 25 (2) (2005) 147–154.
[25] L. Birhanu, B.T. Hailu, T. Bekele, S. Demissew, Land use/land cover change along elevation and slope gradient in highlands of Ethiopia, Remote Sens. Appl.: Soc. Environ. 16 (2019), 100260.
[26] A.B. Aneseyee, E. Elias, T. Soromessa, G.L. Feyisa, Land use/land cover change effect on soil erosion and sediment delivery in the Winike watershed, Omo Gibe Basin, Ethiopia, Sci. Total Environ. 728 (2020), 138776.
[27] H. Kassa, S. Dondeyne, J. Poesen, A. Frankl, J. Nyssen, Impact of deforestation on soil fertility, soil carbon and nitrogen stocks: the case of the Gacheb catchment in the White Nile Basin, Ethiopia, Agric. Ecosyst. Environ. 247 (2017) 273–282.
[28] C.L. van Beek, E. Elias, G.S. Yihenew, H. Heesmans, A. Tsegaye, H. Feyisa, M. Tolla, M. Melmuye, Y. Gebremeskel, S. Mengist, Soil nutrient balances under diverse agro-ecological settings in Ethiopia, Nutrient Cycl. Agroecosyst. 106 (2016) 257–274.

[29] M.B. Moisa, I.N. Dejeneb, I.N.B.B. Merga, D.O. Gemeda, Soil loss estimation and prioritization using geographic information systems and the RUSLE model: a case study of the Anger River sub-basin, Western Ethiopia, J. Water Clim. Change 13 (3) (2022) 1170–1184.
[30] B.G. Sinshaw, A.M. Belete, B.M. Mekonen, T.G. Wubetu, T.L. Anley, W.D. Alamneh, H.B. Atinkut, A.A. Gelaye, T. Bilkew, A.K. Tefera, A.B. Dessie, H.M. Fenta, A. M. Beyene, B.B. Bizuneh, H.T. Alem, D.G. Eshete, S.B. Atanaw, M.A. Tebkew, M.M. Birhanu, Watershed-based soil erosion and sediment yield modeling in the Rib watershed of the Upper Blue Nile Basin, Ethiopia, Energy Nexus 3 (2021), 100023.
[31] B. Gessesse, W. Bewket, A. Bräuning, Model-based characterization and monitoring of runoff and soil erosion in response to land use/land cover changes in the Modjo watershed, Ethiopia, Land Degrad. Dev. 26 (7) (2014) 711–724.
[32] D.T. Meshesha, A. Tsunekawa, M. Tsubo, N. Haregeweyn, Dynamics and hotspots of soil erosion and management scenarios of the Central Rift Valley of Ethiopia, Int. J. Sediment Res. 27 (1) (2012) 84–99.
[33] J. Nyssen, J. Poesen, M. Haile, J. Moeyersons, J. Deckers, H. Hurni, Effects of land use and land cover on sheet and rill erosion rates in the Tigray highlands, Ethiopia, Z. Geomorphol. 53 (2009) 171–197.
[34] N. Haregeweyn, J. Poesen, J. Deckers, J. Nyssen, M. Haile, G. Govers, G. Verstraeten, J. Moeyersons, Sediment-bound nutrient export from micro-dam catchments in northern Ethiopia, Land Degrad. Dev. 19 (2) (2008) 136–152.
[35] A. Haileslassie, J. Priess, E. Veldkamp, D. Teketay, J.P. Lesschen, Assessment of soil nutrient depletion and its spatial variability on smallholders' mixed farming systems in Ethiopia using partial versus full nutrient balances, Agric. Ecosyst. Environ. 108 (1) (2005) 1–16.
[36] G. Singh, R.K. Panda, Grid-cell based assessment of soil erosion potential for identification of critical erosion prone areas using USLE, GIS and remote sensing: acase study in the Kapgari watershed, India, Int. Soil and Water Conserv. Res. 5 (3) (2017) 202–211.
[37] M. Kouli, P. Soupios, F. Vallianatos, Soil erosion prediction using the revised universal soil loss equation (RUSLE) in a GIS framework, chania, northwestern crete, Greece, Environ. Geol. 57 (3) (2009) 483–497.
[38] A.S. Jasrotia, R. Singh, Modeling runoff and soil erosion in a catchment area, using the GIS, in the Himalayan region, India, Environ. Geol. 51 (2006) 29–37.
[39] B.P. Ganasri, H. Ramesh, Assessment of soil erosion by RUSLE model using remote sensing and GIS - a case study of Nethravathi Basin, Geosci. Front. 7 (6) (2016) 953–961.
[40] J. Pascual-Ferrer, Pe′rez-Foguet A, J. Codony, E. Ravento′s, L. Candela, Assessment of water resources management in the Ethiopian Central Rift Valley: environmental conservation and poverty reduction, Int. J. Water Resour. Dev. 30 (3) (2014) 572–587.
[41] J. Nyssen, J. Poesen, M. Haile, J. Moeyersons, J. Deckers, Tillage erosion on slopes with soil conservation structures in the Ethiopian highlands, Soil Tillage Res. 57 (3) (2000) 115–127.
[42] G. Taye, M. Vanmaercke, J. Poesen, B. van Wesemael, S. Tesfaye, D. Teka, J. Nyssen, J. Deckers, N. Haregeweyn, Determining RUSLE P- and C-factors for stone bunds and trenches in rangeland and cropland, North Ethiopia, Land Degrad. Dev. 29 (3) (2017) 812–824.
[43] T. Betru, M. Tolera, K. Sahle, H. Kassa, Trends and drivers of land use/land cover change in Western Ethiopia, Appl. Geogr. 104 (2019) 83–93.
[44] S. Tesfaye, G. Taye, E. Birhane, S.T.M. van der Zee, Spatiotemporal variability of ecosystem water use efficiency in northern Ethiopia during 1982–2014, J. Hydrol. 603 (2021), 126863.
[45] L. Tadesse, K.V. Suryabhagavan, G. Sridhar, G. Legesse, Land use and land cover changes and soil erosion in Yezat watershed, north western Ethiopia, Int. Soil and Water Conserv. Res. 5 (2) (2017) 85–94.
[46] P. Mayaux, H. Eva, A. Brink, F. Achard, A. Belward, Remote sensing of land-cover and land-use dynamics, in: E. Chuvieco (Ed.), Earth Observation of Global Change: the Role of Satellite Remote Sensing in Monitoring the Global Environment, Springer, 2008, pp. 85–108.
[47] M. Biazen, The effect of climate change and variability on the livelihoods of local communities: in the case of central Rift Valley region of Ethiopia, Open Access Libr. J. 1 (4) (2014) 1–10.
[48] T. Molla, B. Sisheber, Estimating soil erosion risk and evaluating erosion control measures for soil conservation planning at Koga watershed in the highlands of Ethiopia, Solid Earth 8 (2017) 13–25.
[49] K. Renard, J. Freimund, Using monthly precipitation data to estimate the R factor in the revised USLE, J. Hydrol. 157 (1–4) (1994) 287–306.
[50] H. Hurni, Erosion-productivity conservation systems in Ethiopia, IV international conference on soil conservation, Maracay Venezuela 674 (1985) 654–674.
[51] D. McCool, G. Foster, C. Mutchler, L. Meyer, Revised slope length factor for the universal soil loss equation, Transactions-of-the-ASAE 32 (5) (1989) 1571–1576.
[52] M. Nearing, A single continuous function for slope steepness influence on soil loss, Soil Sci. Soc. Am. J. 61 (1997) 917–919.
[53] V.L. Durigon, D.F. Carvalho, M.A. Antunes, P.T. Oliveira, M.M. Fernandes, NDVI time series for monitoring RUSLE cover management factor in a tropical watershed, Int. J. Rem. Sens. 35 (2) (2014) 441–453.
[54] J. Nyssen, H. Vandenreyken, J. Poesen, J. Moeyersons, J. Deckers, M. Haile, C. Salles, G. Govers, Rainfall erosivity and variability in the northern Ethiopian highlands, J. Hydrol. 311 (1–4) (2005) 172–187.
[55] D.T. Meshesha, A. Tsunekawa, M. Tsubo, N. Haregeweyn, E. Adgo, Evaluating spatial and temporal variations of rainfall erosivity, case of Central Rift Valley of Ethiopia, Theor. Appl. Climatol. 119 (3–4) (2014) 515–522.
[56] S. Ali, H. Hagos, Estimation of soil erosion using USLE and GIS in Awassa Catchment, Rift valley, Central Ethiopia, Geoderma Regional 7 (2) (2016) 159–166.
[57] B. Bekele, Y. Gemi, Soil erosion risk and sediment yield assessment with universal soil loss equation and GIS: in Dijo watershed, Rift valley Basin of Ethiopia, Model. Earth Syst. Environ. 7 (2021) 273–291.
[58] A. Sharma, K.N. Tiwari, P.B. Bhadoria, P, Effect of land use land cover change on soil erosion potential in an agricultural watershed, Environ. Monit. Assess. 173 (2011) 789–801.
[59] G. Taye, J. Poesen, M. Vanmaercke, B. van Wesemael, L. Martens, D. Teka, J. Nyssen, J. Deckers, V. Vanacker, N. Haregeweyn, V. Hallet, Evolution of the effectiveness of stone bunds and trenches in reducing runoff and soil loss in the semi-arid Ethiopian Highlands, Z. Geomorphol. 59 (4) (2015) 477–493.
[60] L. Bou-imajjane, M.A. Belfoul, R. Elkadiri, M. Stokes, Soil erosion assessment in a semi-arid environment: a case study from the Argana Corridor, Morocco, Environ. Earth Sci. 79 (409) (2020) 1–14.
[61] T. Endalew, D. Biru, Soil erosion risk and sediment yield assessment with revised universal soil loss equation and GIS: the case of nesha watershed, southwestern Ethiopia, Results Geophy. Sci. 12 (2022), 100049.
[62] M. Bagyaraj, B gurugnanam, significance of morphometry studies, soil characteristics, erosion phenomena and landform processes using remote sensing and GIS for kodaikanal hills, A global biodiversity hotpot in western ghats, dindigul district, Tamil nadu, south India, Res. J. Environ. Earth Sci. 3 (3) (2011) 221–233.
[63] D. Tewabe, T. Fentahun, Assessing land use and land cover change detection using remote sensing in the Lake Tana Basin, Northwest Ethiopia, Cogent Environ. Sci. 6 (1) (2020), 1778998.
[64] A. Butt, R. Shabbir, S.S. Ahmad, N. Aziz, Land use change mapping and analysis using Remote Sensing and GIS: a case study of Simly watershed, Islamabad, Pakistan, Egypt. J. Remote Sens. Space Sci. 18 (2) (2015) 251–259.
[65] R.S. Dwivedi, K. Sreeniv, K.V. Ramana, Land-use/land-cover change analysis in part of Ethiopia using Landsat Thematic Mapper data, Int. J. Rem. Sens. 26 (7) (2005) 1285–1287.
[66] R.S. Reid, R.L. Kruska, N. Muthui, A. Taye, S. Wotton, C.J. Wilson, W. Mulatu, Land-use and land-cover dynamics in response to changes in climatic, biological and socio-political forces: the case of southwestern Ethiopia, Landsc. Ecol. 15 (2000) 339–355.
[67] D. Legesse, T. Ayenew, Effect of improper water and land resource utilization on the central Main Ethiopian Rift lakes, Quat. Int. 148 (1) (2006) 8–18.
[68] A. Tilahun, T. Asmare, W. Nega, T. Gashaw, The nexus between land use, land cover dynamics, and soil erosion: a case study of the Temecha watershed, upper Blue Nile basin, Ethiopia, Environ. Sci. Pollut. Res. 30 (2023) 1023–1038.
[69] B.P. Kumar, K.R. Babu, B.N. Anusha, M. Rajasekhar, Geo-environmental monitoring and assessment of land degradation and desertification in the semi-arid regions using Landsat 8 OLI/TIRS, LST, and NDVI approach, Environ. Chall. 8 (2022) 1–11.
[70] Z.H. Shi, L. Ai, X. Li, X. Huang, G.L. Wu, W. Liao, Partial least-squares regression for linking land-cover patterns to soil erosion and sediment yield in watersheds, J. Hydrol. 498 (2013) 165–176.